A Nearly Modern Amphibious Bird from the Early Cretaceous of Northwestern China

Hai-lu You, *et al.*

Science **312**, 1640 (2006);
DOI: 10.1126/science.1126377

Science (print ISSN 0036-8075; online ISSN 1095-9203) is published weekly, except the last week in December, by the American Association for the Advancement of Science, 1200 New York Avenue NW, Washington, DC 20005.

to such indirect dissociations, which is indicated as Scheme C in Fig. 4.

The prediction (*1*) that N(O)–H bond fission after photoexcitation to the $^1\pi\sigma^*$ state represents an efficient nonradiative decay pathway for heteroaromatics like imidazole, pyrrole, and phenol in the gas phase is thus confirmed, irrespective of whether the $^1\pi\sigma^*$ state is populated by direct photoexcitation as in imidazole or pyrrole, or indirectly, by radiationless transfer from a photoprepared $^1\pi\pi^*$ state, as in phenol. The quantum yield for H atom production after UV excitation of pyrrole in the wavelength ranges discussed in this work is estimated to be near unity. Due to the similarity in the PESs for pyrrole and imidazole, we can also assume a high quantum yield for the H atom production in this case. The picture is less clear for phenol, but the fast H atoms formed by the S_1/S_2 coupling at $\lambda <$ 240 nm show anisotropic recoil distributions, implying fast and efficient fragmentation. Further, the recent PTS study of phenol photolysis at 248 nm (*25*) reports no fragmentation channels other than $H + C_6H_5O$ at that wavelength. The available evidence thus suggests that H atom loss is a major process after UV excitation of these gas phase molecules. Future challenges include the following: (i) extending such high-resolution PTS studies to larger, less volatile biomolecules like adenine, histidine, tyrosine, and tryptophan, and (ii) exploring whether such photoinduced prompt N(O)–H bond fission processes also operate in the condensed phase.

References and Notes

1. A. L. Sobolewski, W. Domcke, C. Dedonder-Lardeux, C. Jouvet, *Phys. Chem. Chem. Phys.* **4**, 1093 (2002).
2. L. Serrano-Andrés, M. P. Fülscher, B. O. Roos, M. Merchán, *J. Phys. Chem.* **100**, 6484 (1996).
3. Imidazole, pyrrole, and phenol were obtained commercially (Aldrich, Gillingham, UK, 98%). Pyrrole, at its room temperature vapor pressure (~11 torr) and diluted in 700 torr of Ar, was introduced into the photolysis region in the form of a pulsed, skimmed molecular beam. For imidazole and phenol, solid samples were packed in the tube leading to the same pulsed molecular beam source and heated to ~100°C (imidazole) or 60°C (phenol), and the resulting vapor entrained in 700 torr of Ar before expansion into the interaction region.
4. L. Schnieder, W. Meier, K. H. Welge, M. N. R. Ashfold, C. M. Western, *J. Chem. Phys.* **92**, 7027 (1990).
5. B. Cronin, M. G. D. Nix, R. H. Qadiri, M. N. R. Ashfold, *Phys. Chem. Chem. Phys.* **6**, 5031 (2004).
6. m_H and m_R in Eq. 1 are the masses of the H atom (m_H = 1.0079 dalton) and of the partner fragments (imidazole, pyrrolyl, and phenoxyl, with respective masses m_R = 67.07 dalton, 66.08 dalton, and 93.11 dalton), d = 0.368 m is the length of the flight path, and t is the measured H atom TOF.
7. The angular variation of the product yield is characterized by the beta (β) parameter. Photoexcitation preferentially selects molecules that are aligned so that their transition moment ($\boldsymbol{\mu}$) is parallel to $\boldsymbol{\varepsilon}_{phot}$. Direct dissociation occurs on a time scale that is much shorter than a classical rotational period. The resulting fragments will recoil along the axis of the breaking bond in the photoexcited molecule, i.e., they will display a spatial anisotropy that reflects the original $\boldsymbol{\mu}\cdot\boldsymbol{\varepsilon}$ interaction. The photofragment angular distribution is given by $I(\theta) = [1 + \beta P_2(\cos\theta)]/4\pi$, where θ is the angle between the fragment recoil velocity vector $\mathbf{v}$ and the TOF axis, and $P_2(x) = (3x^2 - 1)/2$ is the second-order Legendre polynomial. β takes limiting values of +2 in the case of prompt dissociation after excitation via a parallel transition (i.e., $\boldsymbol{\mu}$ lies along the breaking bond) and –1 in the case of a perpendicular transition. Less anisotropic fragment recoil distributions (i.e., with β closer to 0) are observed in the case of predissociations (i.e., where the excited state lifetime is comparable to, or longer than, the rotational period of the parent molecule).
8. R. N. Zare, *Angular Momentum. Understanding Spatial Aspects in Physics and Chemistry* (Wiley, New York, 1988).
9. Equilibrium structures and vibrational frequencies discussed in this work were calculated using Gaussian 03 (Revision B.04, M. J. Frisch *et al*., Gaussian, Inc., Pittsburgh, PA, 2003), B3LYP, with a 6-311G(d,p) basis set.
10. Convention identifies the N atom involved in the N–H bond in imidazole as atom 1, and the other heavy atoms in the ring labeled by counting in a clockwise direction in the case of the structure depicted in Fig. 1, i.e., C2, N3, etc.
11. A. J. Gianola *et al.*, *J. Phys. Chem. A* **109**, 11504 (2005).
12. Vibronic coupling is an example of a breakdown of the Born-Oppenheimer separation, which applies when the vibrational and electronic degrees are coupled sufficiently strongly that they cannot be factored. In the case of an electric dipole forbidden transition, inclusion of a quantum of a nonsymmetric vibration changes the overall (vibronic) symmetry and permits the transition (with an intensity that depends on the degree of mixing of the vibrational and electronic wave functions).
13. B. O. Roos, P.-A. Malmqvist, V. Molina, L. Serrano-Andres, M. Merchan, *J. Chem. Phys.* **116**, 7526 (2002).
14. D. A. Blank, S. W. North, Y. T. Lee, *Chem. Phys.* **187**, 35 (1994).
15. J. Wei, A. Kuczmann, J. Riedel, F. Renth, F. Temps, *Phys. Chem. Chem. Phys.* **5**, 315 (2003).
16. J. Wei, J. Riedel, A. Kuczmann, F. Renth, F. Temps, *Faraday Disc* **127**, 267 (2004).
17. H. D. Bist, J. C. D. Brand, D. R. Williams, *J. Mol. Spectrosc.* **24**, 402, 413 (1967).
18. C. Ratzer, J. Kupper, D. Spangenberg, M. Schmitt, *Chem. Phys.* **283**, 153 (2002).
19. A. Sur, P. M. Johnson, *J. Chem. Phys.* **84**, 1206 (1986).
20. R. J. Lipert, S. D. Colson, *J. Phys. Chem.* **93**, 135 (1989).
21. J. Lorentzon, P.-A. Malmqvist, M. Fülscher, B. O. Roos, *Theor. Chim. Acta* **91**, 91 (1995).
22. A. L. Sobolewski, W. Domcke, *J. Phys. Chem. A* **105**, 9275 (2001).
23. Z. Lan, W. Domcke, V. Vallet, A. L. Sobolewski, S. Mahapatra, *J. Chem. Phys.* **122**, 224315 (2005).
24. K. Kimura, S. Nagakura, *Mol. Phys.* **9**, 117 (1965).
25. C.-M. Tseng, Y. T. Lee, C.-K. Ni, *J. Chem. Phys.* **121**, 2459 (2004).
26. S. Ishiuchi *et al.*, *J. Chem. Phys.* **117**, 7077 (2002).
27. K. Daigoku, S. Ishiuchi, M. Sakai, M. Fujii, K. Hashimoto, *J. Chem. Phys.* **119**, 5149 (2003).
28. Two alternative numbering schemes for the normal mode vibrations of benzene and benzene derivatives are commonly found in the scientific literature (the so-called Wilson and Herzberg assignments). We consistently use the former. To assist readers familiar with the latter, the Herzberg labels for the modes of phenol discussed in this work are: $\nu_{16a} \rightarrow \nu_{16}$, $\nu_{16b} \rightarrow \nu_{21}$, $\nu_{18b} \rightarrow \nu_{33}$.

29. We are grateful to the Engineering and Physical Sciences Research Council UK for financial support via the Portfolio Partnership LASER and to K. N. Rosser for his outstanding practical support of this work.

26 January 2006; accepted 24 April 2006
10.1126/science.1125436

A Nearly Modern Amphibious Bird from the Early Cretaceous of Northwestern China

Hai-lu You,[1] Matthew C. Lamanna,[2]* Jerald D. Harris,[3]* Luis M. Chiappe,[4] Jingmai O'Connor,[4] Shu-an Ji,[1] Jun-chang Lü,[1] Chong-xi Yuan,[1] Da-qing Li,[5] Xing Zhang,[6] Kenneth J. Lacovara,[7] Peter Dodson,[8] Qiang Ji[1]

Three-dimensional specimens of the volant fossil bird *Gansus yumenensis* from the Early Cretaceous Xiagou Formation of northwestern China demonstrate that this taxon possesses advanced anatomical features previously known only in Late Cretaceous and Cenozoic ornithuran birds. Phylogenetic analysis recovers *Gansus* within the Ornithurae, making it the oldest known member of the clade. The Xiagou Formation preserves the oldest known ornithuromorph-dominated avian assemblage. The anatomy of *Gansus*, like that of other non-neornithean (nonmodern) ornithuran birds, indicates specialization for an amphibious life-style, supporting the hypothesis that modern birds originated in aquatic or littoral niches.

Neornithean (modern) birds are the most diverse extant tetrapods, comprising ~10,000 species (*1*). Neornitheans, plus the predominantly Late Cretaceous Hesperornithes and *Ichthyornis dispar*, constitute the Ornithurae, a clade that, along with a few other Cretaceous taxa, comprises the Ornithuromorpha (*2*). Previously reported, alleged Early Cretaceous ornithurans are either fragmentary (*3*, *4*), of debatable age (*5*), or have received only limited examination (*6*–*8*). Furthermore, they are rare compared to members of the extinct clade Enantiornithes (*9*, *10*). Consequently, the early evolution of the Ornithuromorpha and the phylogenetic, temporal, and paleoecological contexts of ornithuran (and ultimately neornithean) origins remain obscure. One of the first Early Cretaceous birds discovered was *Gansus yumenensis*, based on an isolated partial left pelvic limb from the Lower Cretaceous (?Aptian-Albian, ~115 to 105 million years ago; see supporting online material) Xiagou Formation near Changma, Gansu Prov-

ince, northwestern China (*11*) (Fig. 1). *Gansus* was initially recognized as more closely allied to neornithean birds than is *Archaeopteryx*; subsequent discoveries have reinforced this hypothesis (*2*, *12*).

Here we describe five new, tern-sized specimens of *G. yumenensis*, also from the Xiagou Formation near Changma, that collectively represent the entire skeleton except the skull, mandibles, and cranial-middle cervical vertebrae (Fig. 2 and figs. S1 to 6). Unlike many compressed or split avian fossils from the Jehol Group of northeastern China, most of the new *Gansus* specimens consist of three-dimensional, largely uncrushed and undistorted bones, and many include soft tissues. Autapomorphies are difficult to pinpoint in the fragmentary *Gansus* holotype, but the most frequently cited feature is pronounced, distally projecting flexor tubercula separate from, and distal to, the proximoplantar ends of the pedal unguals (*10*, *11*). One of the new specimens has identical pedal morphology (Fig. 2J and fig. S5); skeletal elements of this specimen are indistinguishable from their counterparts in the remaining four skeletons, justifying the referral of all to *G. yumenensis*. Unless otherwise noted, the phylogenetically important characters of *Gansus* discussed below represent apomorphies relative to more basal birds (see also supporting online material).

The caudal cervical and 10 thoracic vertebrae of *Gansus* are plesiomorphically not heterocoelous. The thoracics are excavated by deep, emarginate, craniocaudally elongate, lateral pneumatic fossae. The cranialmost three to four thoracics possess well-developed ventral processes ("hypapophyses") (Fig. 2G and fig. S4). The cranialmost three of the 10 to 11 synsacral vertebrae exhibit dorsally directed costal processes. The tail comprises six to seven free vertebrae, all with poorly developed cranial and caudal zygapophyses, and a pygostyle the length of three caudals. All specimens lack ossified gastralia and uncinate processes.

A tall carina extends the length of the sternum (Fig. 2G and fig. S4). Closely spaced coracoidal articular sulci embay the cranial edge of the element. The thin U-shaped furcula has an ~38° intraclavicular angle. The dorsally convex scapula tapers distally. The strutlike, plesiomorphically apneumatic coracoid possesses well-developed procoracoid and lateral processes (Fig. 2E and fig. S2), a deep circular scapular cotyle, and a humeral articular facet situated well ventral to the acrocoracoid process.

The proximal end of the plesiomorphically apneumatic humerus exhibits a ventral tubercle, capital incisure, and domed articular condyle. The cranially projecting bicipital crest bears a transverse sulcus on its proximoventral surface and a tiny fovea caudodistally. A shallow brachial fossa lies proximal to approximately subequal, cranially developed distal humeral condyles. The ulna is slightly longer than the humerus and displays a prominent bicipital tubercle and a deep narrow brachial impression. The dorsal trochlear surface of the dorsal condyle is developed as a semilunate ridge. The carpal trochlea (semilunate carpal) is completely co-ossified with, and positioned proximal to, major and minor metacarpals that may also be fused distally. The weakly developed extensor process of the alular metacarpal extends cranially just beyond the shelflike phalangeal articular facet. The alular metacarpal does not reach the proximal terminus of the intermetacarpal space. The craniocaudal diameter of the major metacarpal is more than twice that of the minor. The proximal phalanx of the major digit is strongly dorsoventrally compressed, flat caudally, and longer than the second phalanx.

The iliac preacetabular alae extend cranially beyond the synsacrum, overlapping the caudalmost pair of thoracic ribs. A weak, subtriangular preacetabular tuberculum ("pectineal process") is situated cranioventral to the acetabulum. A preacetabular ("cuppedicus") fossa is absent. A well-developed antitrochanter occupies the caudodorsal corner of the acetabulum. The pubis and ischium are seamlessly fused to the ilium at the acetabulum. The pubes are strongly retroverted, nearly parallel to the ischia; their distalmost ~5 to 6% are in contact but not fused. The iliac ("dorsal") process of the ischium, situated approximately at midshaft, broadly contacts, and may be co-ossified with, the caudoventral surface of the ilium, enclosing a craniocaudally elongate ilioischiadic foramen (Fig. 2B and fig. S1).

The femur exhibits a trochanteric crest proximolaterally and a patellar sulcus craniodistally. The lateral gastrocnemial ("ectocondylar") tubercle and condyle form a single distolateral trochlear surface. The conjoined cranial and lateral cnemial crests of the tibiotarsus make up a single, well-developed, proximocranially projected rounded crest (Fig. 2C and fig. S1). A tibiotarsal extensor canal is present as an emarginate groove that plesiomorphically lacks a supratendinal pons. The tarsometatarsal articular surface of the approximately subequal distal condyles extends onto the tibiotarsal caudal surface. The fibula terminates proximal to the ankle. The hypotarsus lacks crests and sulci (Fig. 2H and fig. S4). Plantar displacement of the proximal end of metatarsal III creates a deep dorsal extensor sulcus that contains a pronounced tibialis cranialis tuberosity and one vascular foramen that penetrates to the plantar surface. Metatarsal I is twisted and distally deflected so that its plantaromedial surface is concave proximal to its trochlea. The trochlea of metatarsal II lies proximal to the proximalmost extent of those of metatarsals III and IV. It also exhibits marked plantar offset and lateral rotation and is compressed mediolaterally as compared to those of metatarsals III and IV. Metatarsals III and IV completely

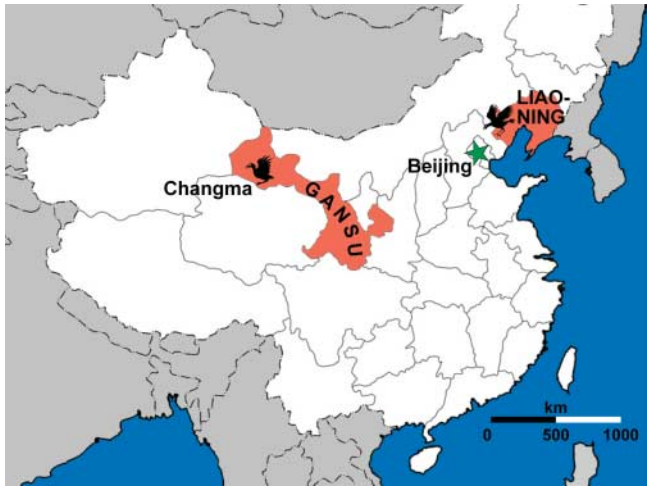

Fig. 1. Map of China (white), with Changma locality in Gansu Province and fossil bird–producing deposits of the Jehol Group in Liaoning Province (~2000 km away) marked by bird silhouettes.

[1]Institute of Geology, Chinese Academy of Geological Sciences, 26 Baiwanzhuang Road, Beijing 100037, People's Republic of China. [2]Section of Vertebrate Paleontology, Carnegie Museum of Natural History, 4400 Forbes Avenue, Pittsburgh, PA 15213–4080, USA. [3]Science Department, Dixie State College, 225 South 700 East, St. George, UT 84770, USA. [4]The Dinosaur Institute, Natural History Museum of Los Angeles County, 900 Exposition Boulevard, Los Angeles, CA 90007, USA. [5]Fossil Research and Development Center, Third Geology and Mineral Resources Exploration Academy of Gansu Province, 1 Langongping Road, Lanzhou, Gansu 730050, People's Republic of China. [6]Provincial Museum of Gansu Province, Nature Department, 3 West Xijin Road, Lanzhou, Gansu 730050, People's Republic of China. [7]Geology and Paleontology Program, Department of Bioscience and Biotechnology, Drexel University, 409 Stratton Hall, 32nd and Chestnut, Philadelphia, PA 19104, USA. [8]Department of Animal Biology, School of Veterinary Medicine, University of Pennsylvania, 3800 Spruce Street, Philadelphia, PA 19104, USA.

*To whom correspondence should be addressed. E-mail: lamannam@carnegiemnh.org (M.C.L); jharris@dixie.edu (J.D.H.)

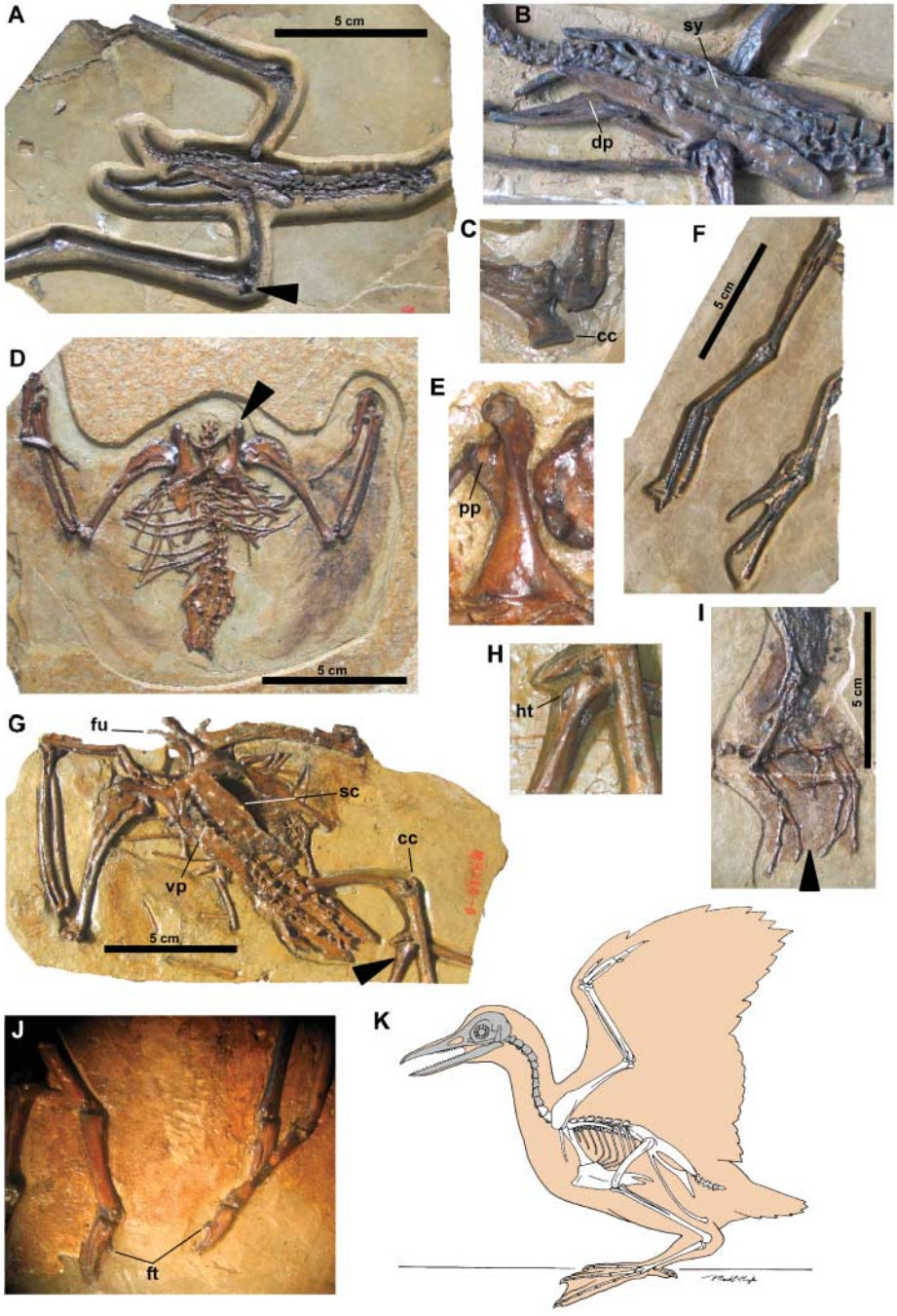

Fig. 2. New specimens of *G. yumenensis* (Chinese Academy of Geological Sciences, Institute of Geology, prefix CAGS-IG-04-). (**A**) CM-002, articulated caudal cervical, thoracic, synsacral, and caudal vertebrae, pelvic girdle, and partial pelvic limbs in right dorsolateral view. (**B**) CM-002, pelvis and synsacrum. (**C**) CM-002, proximal right tibiotarsus [indicated by arrowhead in (A)]. (**D**) CM-004, nearly complete skeleton in ventral view with feathers (dark brown) on thoracic limbs, lacking cranium, cranial-midcervical vertebrae, and both pelvic limbs. (**E**) CM-004, left coracoid in ventral view [indicated by arrowhead in (D)]. (**F**) CM-001, partial right and left pelvic limbs. (**G**) CM-003, nearly complete skeleton in ventral view, lacking cranium, cervical vertebrae, distal left thoracic limb, and right and distal left pelvic limbs. (**H**) CM-003, proximal tarsometatarsus [indicated by arrowhead in (G)]. (**I**) CM-008, partial pelvic limbs with soft-tissue preservation. (**J**) CM-008, tubercular soft tissue preserved around toes [indicated by arrowhead in (I)]. (**K**) Reconstruction of *G. yumenensis* based on new specimens. Elements shaded gray remain unknown. Abbreviations in figure are as follows: cc, cnemial crests; ft, flexor tubercula; dp, dorsal process of ischium; fu, furcula; ht, hypotarsus; pp, procoracoid process; sc, sternal carina; sy, synsacrum; vp, ventral processes of cranial thoracic vertebrae.

enclose a large, proximodistally elongate, distal vascular foramen. The first phalanges of all pedal digits are longer than any of their respective distal phalanges; all unguals are small, short, and unrecurved.

Wing feathers preserved with one specimen (Fig. 2D and fig. S2) are asymmetrical and virtually identical to those of volant modern birds. Semiplumes or down also appear to be present.

Most Early Cretaceous bird species have been recovered from northeastern China and Spain and are primarily non-ornithuromorphs (enantiornitheans plus more basal taxa) (*8*, *10*, *13*). However, most of nearly 50 bird specimens recovered from Changma appear to pertain to *Gansus*. Thus, the Xiagou Formation preserves the oldest known avian assemblage dominated by ornithuromorphs, possibly indicating the first stages of the rise of ornithuromorphs to diversity-based dominance over enantiornitheans (supporting online material).

Despite pectoral and alar features that indicate powered flight, *Gansus* pelvic limb elements exhibit specializations that are characteristic of amphibious (*14*) birds. Osteologically, these include the prominent, proximally projecting cnemial crests on the tibiotarsus; proximal position of the trochlea of metatarsal II; elongate pedal digits [III and IV each longer than the tarsometatarsus (tables S1 and S2)] with elongate proximal phalanges (all longer than any penultimate phalanges); and unrecurved unguals with large flexor tubercula. Except the last, these features predominantly occur elsewhere in undoubted foot-propelled divers such as *Hesperornis*, loons (Gaviidae), and grebes (Podicipedidae) (*15*); the cnemial crests are more elongate in *Gansus* than in the slightly younger hesperornithean *Enaliornis* (*5*). Similar flexor tubercula characterize some extant shorebirds (Charadriiformes) (*3*), herons (Ardeidae), and diving ducks (Anatidae) (*16*). Moreover, one new *Gansus* specimen preserves tubercular skin surrounding the pedal digits (Fig. 2J and fig. S5) that indicate interdigital telae (webbing) extending at least to the proximal ends of the unguals. The presence of web-footed birds in the Early Cretaceous is supported by footprints elsewhere in Asia (*17*). *Gansus* has typically been considered a sandpiper (Scolopacidae) analog (*3*, *11*), implying that it was not amphibious (that is, it lacked fully webbed feet and did not dive) but instead waded and probed nearshore sediments for food (*1*). Its anatomy, however, demonstrates that it was more similar to, but not as adept as, foot-propelled diving birds such as grebes, loons, and diving ducks.

In all consensus trees from a phylogenetic analysis (see supplementary online material for methods and details), *Gansus* occurs with-

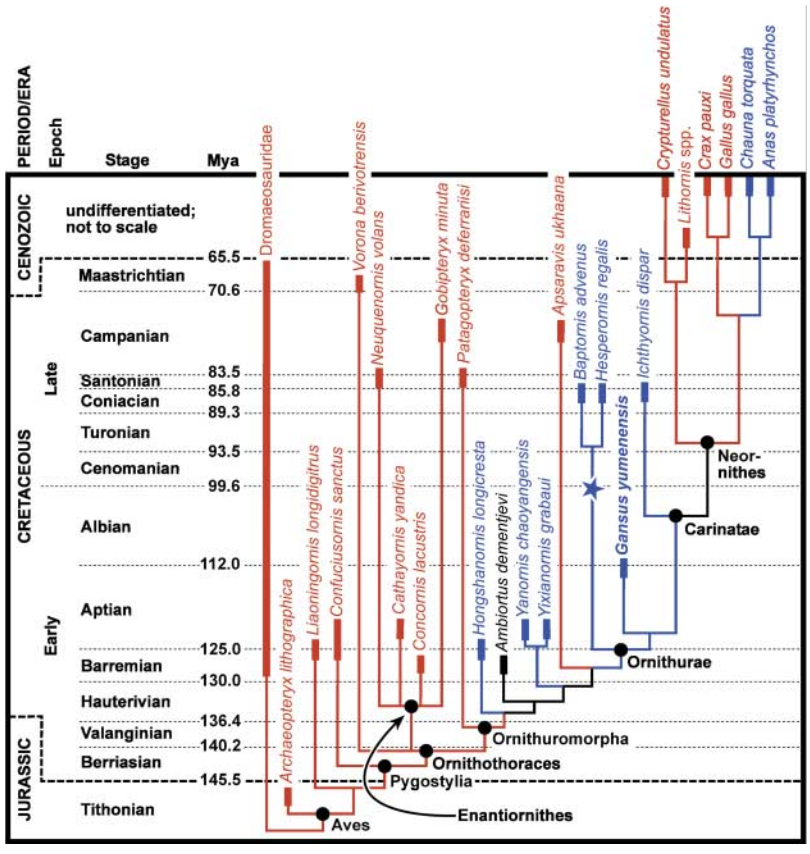

Fig. 3. Phylogenetic position of *G. yumenensis* (50% majority-rule consensus tree) based on holotype and new referred specimens; time scale is per (*28*). Thin line segments represent ghost lineages; thick line segments represent known ranges of terminal taxa. Clades are denoted by black circles (see supporting online material for clade definitions). The star represents the temporal position of *Enaliornis* spp. Colors indicate known or inferred ecologies as follows: brown, terrestrial/arboreal; blue, aquatic/amphibious; black, equivocal. Note the sequence of amphibious taxa basal to the Neornithes. Depicted divergence times are intended as approximations only, based on the oldest occurrence of an included species and subsequent divergences. Mya, million years ago.

in the Ornithurae (Fig. 3). This position is considerably more derived than that of all known birds from the Jehol Group of northeastern China. *Gansus* predates other, later Cretaceous ornithurans that are considered to exhibit amphibious features [such as hesperornitheans] or are thought to have occupied water-based niches [such as *Ichthyornis*] (*5*, *12*, *18*–*23*). Some younger yet more basal ornithuromorphs, including *Apsaravis ukhaana* (*24*) and *Patagopteryx deferrariisi* (*25*), occupied fully terrestrial niches, as did some later purported neornitheans (*12*, *20*, *24*). *Ichthyornis* and *Gansus* are recovered as proximal outgroups to the Neornithes, consistent with the hypothesis that neornitheans originated in an aquatic habitat (*26*). Thus (Fig. 3), the most basal ornithuromorphs appear to have evolved in a terrestrial/arboreal context (*25*) but rapidly shifted to an aquatic ecology (*8*) (Fig. 3).

Before the end of the Cretaceous, some non-ornithuran ornithuromorphs must have reverted to a terrestrial life-style (*24*). The Cretaceous existence of members of basal neornithean clades [Anseriformes and possibly Gaviiformes (*19*, *20*, *22*)] implies that representatives of the neornithean clades Galliformes and more basal Palaeognathae, all known fossil and extant members of which are terrestrial, must also have existed during the Cretaceous (*27*). Thus, although neornitheans may have originated in aquatic niches, some basal neornitheans apparently re-radiated into terrestrial niches before the Cretaceous/Paleogene extinction event. Consequently, contrary to recent hypotheses, adaptation to an aquatic ecology appears to have played little part in the survival of birds across the K/P boundary (*27*).

References and Notes

1. F. B. Gill, *Ornithology* (Freeman, New York, ed. 2, 1995).
2. L. M. Chiappe, in *Mesozoic Birds: Above the Heads of Dinosaurs*, L. M. Chiappe, L. M. Witmer, Eds. (Univ. of California Press, Berkeley, CA, 2002), pp. 448–472.
3. L. Hou, *Mesozoic Birds of China* (Feng-huang-ku Bird Park, Taiwan, 1997) (in Chinese).
4. E. N. Kurochkin, *Smithson. Contrib. Paleobiol.* **89**, 275 (1999).
5. P. M. Galton, L. D. Martin, in *Mesozoic Birds: Above the Heads of Dinosaurs*, L. M. Chiappe, L. M. Witmer, Eds. (Univ. of California Press, Berkeley, CA, 2002), pp. 317–338.
6. C. Yuan, *Acta Geol. Sin.* **78**, 464 (2004) (in Chinese with English summary).
7. Z. Zhou, F. Zhang, *Chin. Sci. Bull.* **46**, 1258 (2001).
8. Z. Zhou, F. Zhang, *Proc. Natl. Acad. Sci. U.S.A.* **102**, 18998 (2006).
9. L. Hou, Z. Zhou, F. Zhang, Y. Gu, *Mesozoic Birds from Western Liaoning in China* (Liaoning Science and Technology Publishing House, 2002) (in Chinese).
10. Z. Zhou, L. Hou, in *Mesozoic Birds: Above the Heads of Dinosaurs*, L. M. Chiappe, L. M. Witmer, Eds. (Univ. of California Press, Berkeley, CA, 2002), pp. 160–183.
11. L. Hou, Z. Liu, *Sci. Sin. Ser. B* **27**, 1296 (1984).
12. S. Hope, in *Mesozoic Birds: Above the Heads of Dinosaurs*, L. M. Chiappe, L. M. Witmer, Eds. (Univ. of California Press, Berkeley, CA, 2002), pp. 339–388.
13. J. L. Sanz, B. P. Pérez-Moreno, L. M. Chiappe, A. D. Buscalioni, in *Mesozoic Birds: Above the Heads of Dinosaurs*, L. M. Chiappe, L. M. Witmer, Eds. (Univ. of California Press, Berkeley, CA, 2002), pp. 209–229.
14. V. de Buffrénil, J.-M. Mazin, in *Secondary Adaptations of Tetrapods to Life in Water*, J.-M. Mazin, V. de Buffrénil, Eds. (Friedrich Pfeil, Munich, Germany, 2001), pp. 91–93.
15. J. Cracraft, *Syst. Zool.* **31**, 35 (1982).
16. R. W. Shufeldt, *N.Y. State Mus. Bull.* **130**, 5 (1909).
17. J.-D. Lim, Z. Zhou, L. D. Martin, K.-S. Baek, S.-Y. Yang, *Naturwissenschaften* **87**, 256 (2000).
18. O. C. Marsh, *Prof. Pap. Eng. Dept. U.S. Army* **18**, 1 (1880).
19. E. N. Kurochkin, G. J. Dyke, A. A. Karhu, *Am. Mus. Novit.* **3386**, 1 (2002).
20. S. Chatterjee, in *Proceedings of the 5th Symposium of the Society of Avian Paleontology and Evolution, Beijing, 1-4 June 2000*, Z. Zhou, F. Zhang, Eds. (Science Press, Beijing, China, 2002), pp. 125–155.
21. D. C. Parris, S. Hope, in *Proceedings of the 5th Symposium of the Society of Avian Paleontology and Evolution, Beijing, 1-4 June 2000*, Z. Zhou, F. Zhang, Eds. (Science Press, Beijing, China, 2002), pp. 113–124.
22. J. A. Clarke, C. P. Tambussi, J. I. Noriega, G. M. Erickson, R. A. Ketcham, *Nature* **433**, 305 (2005).
23. G. J. Dyke *et al.*, *Naturwissenschaften* **89**, 408 (2002).
24. J. A. Clarke, M. A. Norell, *Am. Mus. Novit.* **3387**, 1 (2002).
25. L. M. Chiappe, in *Mesozoic Birds: Above the Heads of Dinosaurs*, L. M. Chiappe, L. M. Witmer, Eds. (Univ. of California Press, Berkeley, CA, 2002), pp. 281–316.
26. A. Feduccia, *Trends Ecol. Evol.* **18**, 172 (2003).
27. D. S. Robertson, M. C. McKenna, O. B. Toon, S. Hope, J. A. Lillegraven, *Geol. Soc. Am. Bull.* **116**, 760 (2004).
28. F. M. Gradstein, J. G. Ogg, A. Smith, *A Geologic Time Scale 2004* (Cambridge Univ. Press, Cambridge, 2004).

29. We thank Z.-c. Bai. and C. Peng and their field crew for excavation and collection of the specimens; G.-h. Cui and Y.-q. Zhang for specimen preparation; B. Livezey, Z.-x. Luo, and R. Mulvihill for discussion; S. Yu for translating (*6*); M. Klingler for Fig. 2K; and anonymous manuscript reviewers. Funding was provided by the Discovery Quest program for The Science Channel to H.-l.Y., M.C.L., and J.D.H.; the Carnegie Museum of Natural History to M.C.L.; Dixie State College to J.D.H.; the Chinese Geological Survey of the Ministry of Land and Resources of China and the Ministry of Science and Technology of China (973 Project) to H-l.Y. and Q.J.; and the Gansu Bureau of Geology and Mineral Resources to D.-q.L.

Supporting Online Material

www.sciencemag.org/cgi/content/full/312/5780/1640/DC1
Materials and Methods
SOM Text
Figs. S1 to S6
Tables S1 and S2
References

17 February 2006; accepted 19 April 2006
10.1126/science.1126377